PREDICTION OF PERMEABILITY OF ORDERED AND DISORDERED TWO-DIMENSIONAL POROUS MEDIA IN THE DARCY REGIME USING THE LATTICE BOLTZMANN METHOD

Cirilo Seppi Bresolin, cirilo@labcet.ufsc.br
Amir Antônio Martins de Oliveira, amir.oliveira@gmail.com
Universidade Federal de Santa Catarina, Florianópolis, SC CEP 88120-900

Abstract. *Lattice Boltzmann methods allow for the treatment of fluid flow in complex geometries, such as porous media, with significantly less computational time when compared to finite volume or finite element algorithms. Here, a prediction of the Darcy permeability for single-phase flow in two-dimensional particulated ordered and disordered porous media using LBM is presented. Differently from previous work, a collision operator with a Two Relaxation-Time scheme is used instead of the usual BGK approximation. The results for ordered arrays of aligned and staggered circular cylinders are compared to results from previous investigations showing excellent agreement. Random porous media are generated by randomly positioning circular, square and rectangular cross section solid particles, for porosities between 0.50 and 0.95. Using the LBM-TRT model it is shown that all arrangements result in approximately the same relationship between porosity and permeability for the range of permeability analyzed, except for rectangular inclusions aligned with the flow direction. These present lower permeability for the calculated range. It is concluded that the Darcy permeability presents strong dependency on the shape of the inclusion only for cross sections with large aspect ratios, when particle-induced anisotropic flow effects become pronounced.*

Keywords: *Lattice Boltzmann Method, Two Relaxation Times, Permeability, Array of Cylinders, Porous Media*

1. Introduction

The analysis of flows through complex geometries is based commonly in two different approaches: Either (1) point-wise detailed solutions using the macroscopic continuum equations or (2) volume and time (or ensemble) averaged equations are used. The former approaches are particularly powerful when addressing problems that are geometrically simple. The latter, however, are basically the only choices when one attempts to solve problems in geometries closer to the applications. In the averaged formulations, detailed information is lost in the averaging procedure, giving rise to the effective transport properties that are usually modeled using empirical data.

In recent years, the development of Lattice-Boltzmann methods (LBM) have become an alternative for treatments based on the continuum transport equations. The LBM is a numerical scheme to solve the Boltzmann Equation in a mesoscale approach. The LBM has been preferable to simulate flow in complex geometries, such as porous media because, a priori, it independents of empirical models for the effective transport properties.

The fluidynamic permeability is a measure of flow conductance through a porous matrix. It is defined from the relation between the average flow speed and the pressure gradient or body force that drive it. Darcy's equation relates the permeability tensor with the averaged superficial velocity vector as

$$\vec{U}_D = -\frac{\overline{\overline{K}}}{\mu} \cdot \vec{\nabla} P \tag{1}$$

where $\overline{\overline{K}}$ is the permeability tensor. The Darcy equation is valid only for pore (or particle) Reynolds numbers in the creeping flow regime, i.e., $Re_d << 1$ where d is the particle diameter.

Early models for the permeability, such as the hydraulic radius, statistical and viscous drag models Scheidegger (1974); Dullien (1979); Kaviany (1995) have stressed the fact that the saturated permeability depends only on the topology of the pore space, being independent of the fluid properties for Newtonian incompressible fluids in the absence of local electromagnetic and chemical effects.

Previous work reporting permeability of porous media have relied on direct measurement Eidsath *et al.* (1983); Sadiq *et al.* (1995); ensemble averaging Torquato and Beasley (1997); variational methods Torquato (1990); Torquato and B. Lu (1990); homogenization Wang *et al.* (2003); Boutin and Geindreau (2008);Mityushev and Adler (2002); Tamayol and Bahrami (2009); eigenfunction expansion and domain decomposition Wang (1996, 2001);finite volume and finite element methods Lee and Yang (1997); Sahraoui and Kaviany (1994); Sangani and Acrivos (1982); Petrasch *et al.* (2008); Sobera and Kleijn (2006); and LBM solutions Belov *et al.* (2004); Clague *et al.* (2000); Manwart *et al.* (2002); Nabovati *et al.* (2009); Santos *et al.* (2002), among others. The results from the many simpler models vary by many orders of magnitude even when detailed statistical information on the topology of the porous structure is available Petrasch *et al.* (2008). As a result, the rigorous determination of the permeability and the study of the effect of the many topological parameters that characterize the porous structure depends on direct point-wise simulation of the flow supported by direct measurement on

those configurations that can, technically and economically, be reproduced in laboratory. This research strategy may lead to the development and optimization of new combustion systems, chemical sensors, microfluidic and energy-conversion devices. Methods based on the solution of the Boltzmann Transport Equation appear as a powerful framework to address these problems.

In this direction for the development of efficient structures for the many applications, the LBM with Two Time Relaxation model as the collision operator is used to study the permeability in ordered and disordered 2D geometries with isothermal transverse flow. First, a simulation of the flow in parallel channels is presented to compare the TRT and BGK schemes. Then, a study of the flow through an array of cylinders disposed in aligned and in staggered configurations is presented and the results are compared to previous available numerical results obtained with different methods. Finally, the method is applied to study disordered porous media with different solid cross-sectios, with a focus on the effect of flow anisotropy induced by the particle shape.

2. The Lattice Boltzmann Method

The LBM evolved from the lattice gas automata (McNamara and Zanetti, 1988) and can also be derived directly from the Boltzmann equation (He and Luo, 1997; Abe, 1997; Philippi *et al.*, 2006; Shan *et al.*, 2006). Basically, it uses a finite difference scheme to solve the space and time parts of the continuous Boltzmann equation. The moments of the distribution function are the macroscopic fluid-dynamic variables (density, velocity, energy). To integrate the moments, a Hermite-Gauss quadrature scheme is used. The collision operator is generally approximated using the BGK model (Bhatnagar *et al.*, 1954). It had been shown by Pan *et al.* (2006) that the BGK model have some drawbacks as the permeability dependence on viscosity and the position of the wall when using the bounce-back scheme as no-slip boundary condition. To overcome these drawbacks (Ginzburg and d'Humières, 2003; d'Humières and Ginzburg, 2009) suggests the two time relaxation model.

2.1 The isothermal fluid-dynamic model with two relaxation times collision operator

The TRT model is based on the decomposition of the population solution into its symmetric and anti-symmetric components. Each of these components has its own relaxation times that with the proper choice of values eliminate the principal drawbacks of the BGK.

The discretization of the Boltzmann equation generates a set of particle populations, that follow a Maxwellian distribution function. This set of populations follow the evolution equation,

$$f_\alpha(\vec{r}+\vec{e}_\alpha, t+1) - f_\alpha(\vec{r}, t) = \Omega \tag{2}$$

where $\vec{r}$ is the position vector, t is the time, $\vec{e}_\alpha$ is the set of velocity vectors, Fig. 1, that defines the lattice grid and over which the f_α populations are distributed, Ω is the collision operator that on the TRT model has two parts, one called symmetric "+" and another called anti-symmetric "-". Their definitions follows as,

$$\Omega = -\Omega^+ \ - \Omega^- \tag{3}$$

$$\Omega^\pm = \omega^\pm \ \left[f_\alpha^\pm(\vec{r}, t) - f_\alpha^{eq,\pm}(\vec{r}, t)\right] \tag{4}$$

$$f_\alpha^\pm = \frac{f_\alpha(\vec{r}, t) \pm f_{\bar{\alpha}}(\vec{r}, t)}{2} \tag{5}$$

$$f_\alpha^{eq,\pm} = \frac{f_\alpha^{eq}(\vec{r}, t) \pm f_{\bar{\alpha}}^{eq}(\vec{r}, t)}{2} \tag{6}$$

where f_α^{eq} is the equilibrium distribution function, and the subscript $\bar{\alpha}$ represents the opposite velocity vector of α, see Fig 1, $\omega^\pm$ are the relaxation frequencies for the symmetrical and antisymmetric parts. There are a series of "magic" proportions between the relaxation frequencies that should be respect to guarantee the method stability. Herein the relation used between then is

$$\omega^- = \frac{8(2-\omega^+)}{8-\omega^+} \tag{7}$$

this relation was choose because guarantees that the wall is place correctly between a wall and fluid node in the bounce-back scheme for non-slip wall (discussed below). If $\omega^- = \omega^+$ the TRT reduces to the Single Relaxation Time model, BGK,

$$\Omega = \omega \ [f_\alpha(\vec{r}, t) - f_\alpha^{eq}(\vec{r}, t)] \tag{8}$$

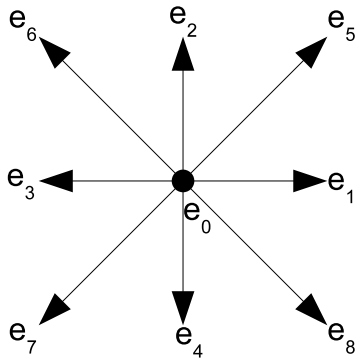

Figure 1: The 9 velocity vectors $\vec{e}_\sigma$ of the lattice grid D2Q9.

At every time step, the set of populations are propagated and relaxed. The propagation consists in moving each population in its respective direction to the neighbor lattice element. The relaxation consists in updating the population value, relaxing it toward the equilibrium distribution function. The equilibrium distribution function is the Maxwellian distribution function expanded in a Taylor series and for low Mach number, it can be written as,

$$f_\alpha^{eq} = w_\alpha \rho \left\{ 1 + 3\vec{e}_\alpha \cdot \vec{u} + \frac{9(\vec{e}_\alpha \cdot \vec{u})^2}{3} - \frac{3\vec{u}^2}{2} \right\} \tag{9}$$

where w_α are weighting factors. The factors for D2Q9 lattice shown in Fig. 1 are $w_0 = \frac{4}{9}$, $w_{1,2,3,4} = \frac{1}{9}$, $w_{5,6,7,8} = \frac{1}{36}$.

The macroscopic variables, density and velocity are the moments of the distribution function, that after the Hermite-Gauss integration result in the following summations,

$$\rho = \sum_\alpha f_\alpha \tag{10}$$

$$\rho\, \vec{u} = \sum_\alpha \vec{e}_\alpha\, f_\alpha \tag{11}$$

The Hermite-Gauss integration defines the number of populations. Since for in the isothermal hydrodynamic model only the first, second and third moments of the distribution function need to be correctly recovery, the 9 populations lattice (D2Q9) produces a third order error in the macroscopic velocity in the Navier Stokes equations.

From the perfect gas equation, the pressure is,

$$p = \frac{\rho}{3} \tag{12}$$

The sound speed, c_s, then become $\sqrt{1/3}$. Applying the Chapman-Enskog expansion to Eq. 2, it is possible to recover the Navier-Stokes equations. From the expansion, the relation between the relaxation frequency parameter and kinematic viscosity appear as,

$$\nu = \left(\frac{1}{\omega_s} - \frac{1}{2} \right) \frac{1}{3}. \tag{13}$$

The no-slip boundary condition is applied using a bounce-back scheme. It consists in reverting the populations on the wall sites of the lattice during the propagation step, e.g., $f_1 \rightarrow f_3$, $f_5 \rightarrow f_7$ $f_8 \rightarrow f_6$ for a vertical wall with $\vec{n} = (-1, 0)$. This simple scheme is what make the LBM suitable to simulate complex geometries, as porous media. The drawback of the bounce-back in the BGK scheme is that the error increase if the relaxation frequency parameter is not close to 1.0 Noble *et al.* (1995). Other boundary conditions, as those related to velocity and pressure are discussed by Zou and He (1997).

3. Results

The LBM algorithm was implemented in Fortran 95. The porous medium was generated as a bitmap image that could be drawn in any drawing software, such as Microsoft's Paint. These bitmap images are read and interpreted by the computer code, that assigns black pixels as solid phase and white pixels as fluid phase. The image pixel resolution are the lattice dimensions. For simulations with different porosities, different bitmap images were generated using different particles radii, but with the same lattice dimensions. For the simulation of disordered porous media, a code that generates

random distributions of solid particles with the desired porosity was implemented. This scheme used to build lattices has been handy, because it is easy to deal with bitmap images and no effort was spent in programing a generator for the porous media of interest.

Initially, the Poiseuille flow along a bunch of channels formed by parallel plates is simulated to compare the results from the TRT and BGK schemes. Then, the flow in ordered porous media formed by aligned arrangement of parallel cylinders is solved and the results are compared to correlations. Finally the flow in random porous media formed by particles with different cross-sections is solved to determine the effect of particle shape and orientation on permeability.

3.1 Comparison between BGK and TRT collision models

Figure 2 presents a rendering of a channel formed by a bunch of parallel flat tubes. The lattice has the dimensions of 65 x 100 lattice units in height and length, respectively, and the fluid density is set equal to 1.0. In the TRT simulations, the symmetrical relaxation frequency was varied from 0.7 to 1.3, and the relation Eq. 7 was used to set the anti-symmetrical relaxation frequency. For the BGK simulations both relaxation frequencies were set equal. A pressure gradient was imposed as a body force equal to 1.0×10^{-7}. For this condition, $Re_d << 1$, situating the flow in a Darcy regime. Periodic boundary conditions are set at the inlet and outlet of the channel, producing a fully developed flow condition. The simulation is run for 200,000 iterations to achieve steady state. The results are depicted in Fig. 3.

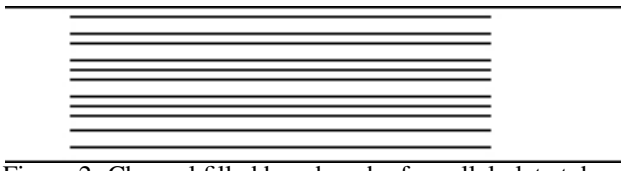

Figure 2: Channel filled by a bunch of parallel plate tubes.

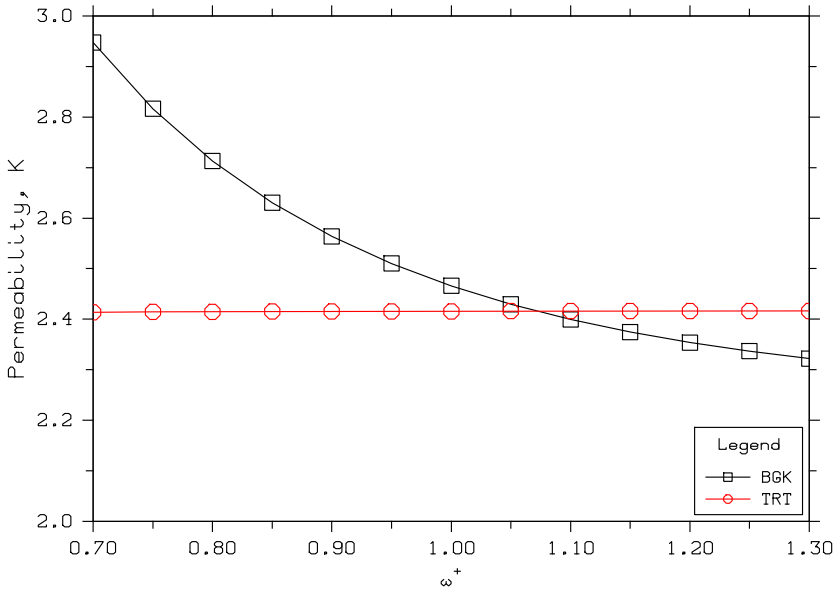

Figure 3: Solution for the Poiseuille flow along parallel flat plates, comparing the BKG and TRT schemes for the collision operator.

It can be seen from Fig. 3 that the permeability is constant with the relaxation frequency in the TRT model, while it changes in the BGK model depending on the choice of the single relaxation parameter. The point where the curves cross is $\omega^+ = 1.07$. At this value, $\omega^+ = \omega^-$ in Eq. 7 and the TRT reduces to the BGK model. The TRT model will be used from here on.

3.2 Ordered porous media

For the simulation of ordered porous media, unit cells representing arrays of aligned and staggered cylinders are used, Fig. 4. Since the boundary conditions are all periodic, it is possible to solve for only one cylinder in the aligned array, as shown in Fig. 4a. However, using four cells the convergence became more stable and the simulations less prone to diverge. The unit cell has the dimensions of 256 x 256 lattice units and the cylinders radii are varied to recover the desired porosity. The porosity was varied from 30% to 95%, with 5% steps. The lower bound of 30% is closer to the condition of

point contact. The simulation was run for 100,000 iterations. To impose the pressure gradient, a body force was set equal to 1×10^{-7}. These values resulted in $Re_d << 1$, ensuring the Darcy flow regime. From the velocity field, the mean pore velocity $\bar{u}_p$ is calculated. Then, the Darcy velocity $U_D = \bar{u}_p \varepsilon$ is obtained. The value of permeability is then calculated from Eq. 1.

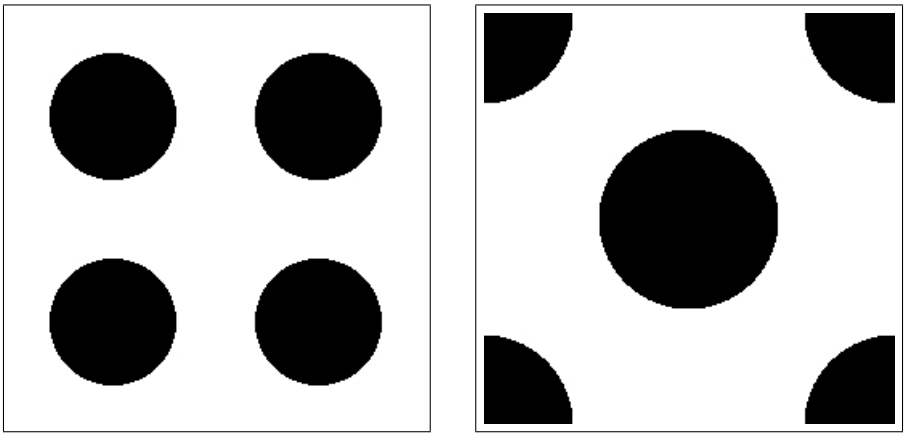

(a) Aligned (b) Staggered

Figure 4: Unit cells for porosity of 70%: (a) Alligned and (b) staggered arrangements.

Figure 5 presents the results for aligned and staggered arrangements of cylinders obtained with the LBM-TRT model. The permeability is nondimensionalized in respect to the particle diameter d. The results for aligned cylinders are compared to solutions from other authors available in the literature. The results for aligned cylinders present excellent agreement with the results of Sangani and Acrivos (1982) over the entire range of porosity. When compared to the results of Sobera and Kleijn (2006) and Kaviany (1995), the present results show better agreement for high values of porosity, while when compared to Tamayol and Bahrami (2009), there is better agreement in the low porosity range. The deviation from the work of Kaviany (1995) is mainly because their correlation was developed for the range of porosity from 40% to 80%, so the upper and lower branches are extrapolations. The deviation of Sobera and Kleijn (2006) at high porosity is, as stated by the authors, due the change in the scaling factor behavior. At high volume fraction, the lenght scale over which rapid changes occur is $\sqrt{\delta d}$ rather then d, where δ is the half space between two cylinders. The deviation to the results by Tamayol and Bahrami (2009) is probably due to the fact that the assumed parabolic velocity profile among the cylinders with $u_b = 0.0$. Where the u_b is the velocity in the center line of two cylinders in the same row. Even applying the suggested correction, that the u_b is a linear function of u_{max} in the center line of unit cell, the agreement is not better. The permeability for the array of staggered cylinders is equal to the permeability for aligned cylinders over the entire range of porosity, because the staggering of the rows do not perturb the creeping flow. Thus, essentially the cylinders do not feel the presence of each other.

3.3 Disordered porous media

Disordered porous media formed by a random arrangement of cylinders with different cross sections, square, circular and rectangular, were generated, as shown in Fig. 6. The unit cells are generated as bitmap images with porosities from 50% to 95%. Below 50%, the pores are closed and there is no percolation. The position of the center of the solid cylinders was kept the same for all cross sections, as it can be seen comparing Figs. 6a and 6b. Then, all unit cells share basically the same tortuosity defined in the hydraulic radius models Kaviany (1995). The cross-section area of each solid link is kept the same, $A = 64ld^2$ where ld is the lattice unit of distance, regardless of the shape. The porosity is varied increasing the particle density in the lattice. The particles with rectangular shape, with aspect ratio equal to 4, may have the longest side aligned or transversal to the direction of the primary flow. The simulation conditions are the same as for the ordered media.

The results are presented in Fig. 7. The permeability is nondimensionalized in respect to the unit cell main length L. It can be seen that for disordered porous media the permeability is basically independent of the shape of the solid cylinders, as long as the medium remains isotropic. The largest difference is observed between the results for the vertical and horizontal rectangles. The anisotropy of the porous structures reflects in different flow conditions for the aligned and the transversal arrangement of rectangular cylinders. The porous media with plate like cylinders present an anisotropic permeability tensor.

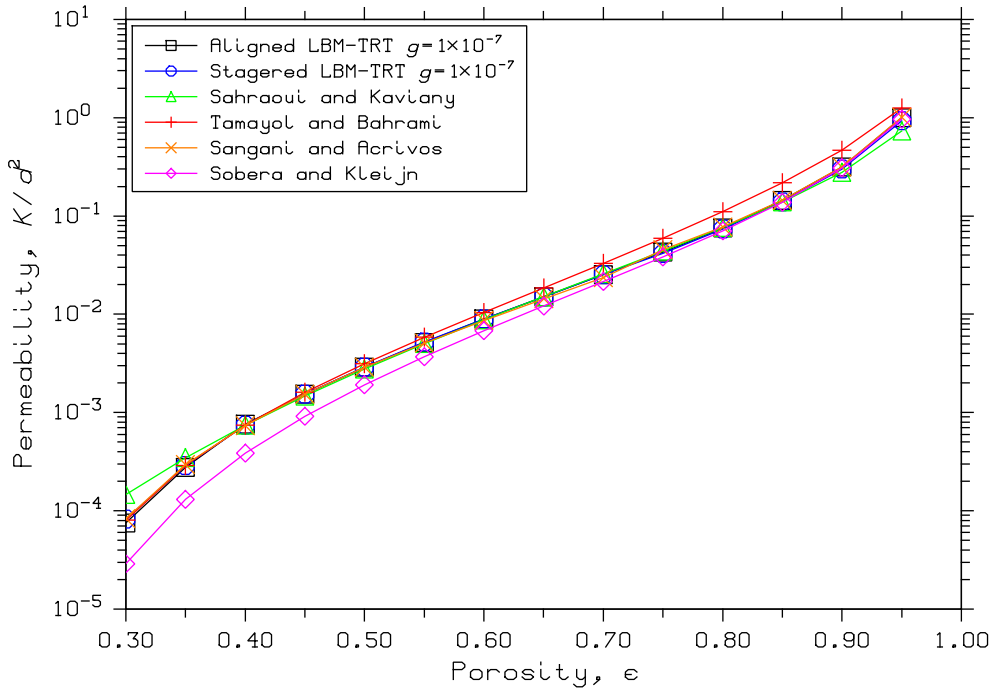

Figure 5: Results of permeability for arrays of aligned and staggered cylinders as a function of porosity. The results of other authors are for aligned cylinders only.

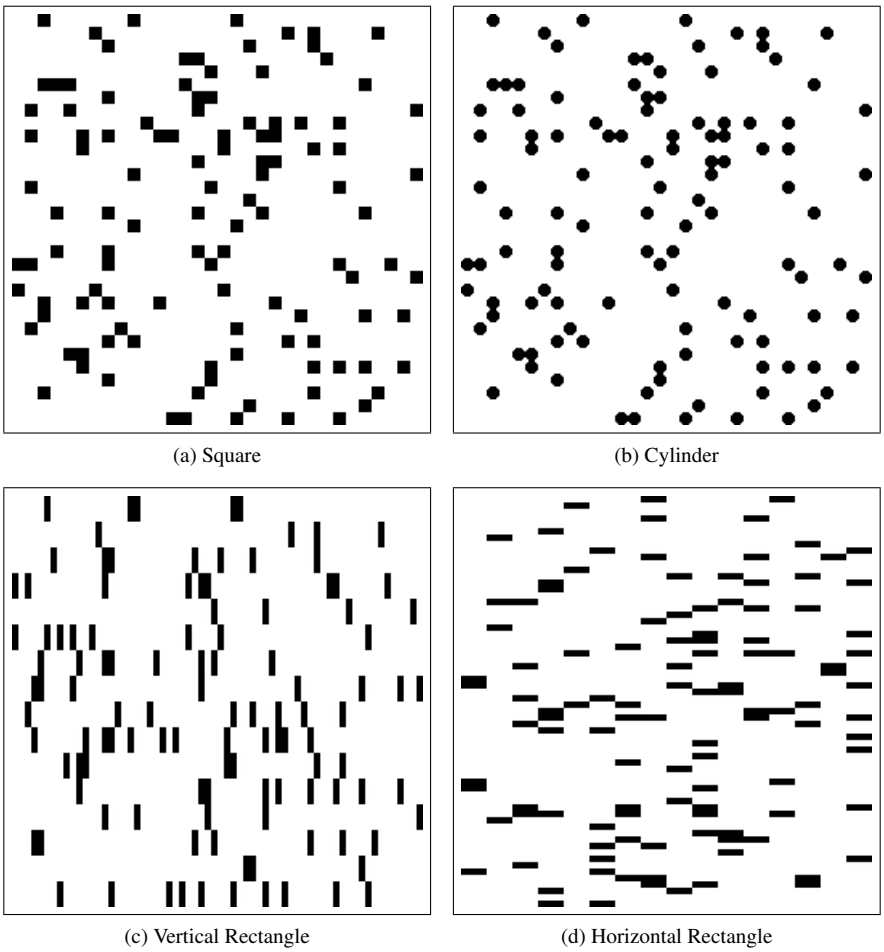

(a) Square (b) Cylinder

(c) Vertical Rectangle (d) Horizontal Rectangle

Figure 6: Unit cells for disordered porous media: Square, circular and rectangular cross sections. The primary flow direction is from left to right.

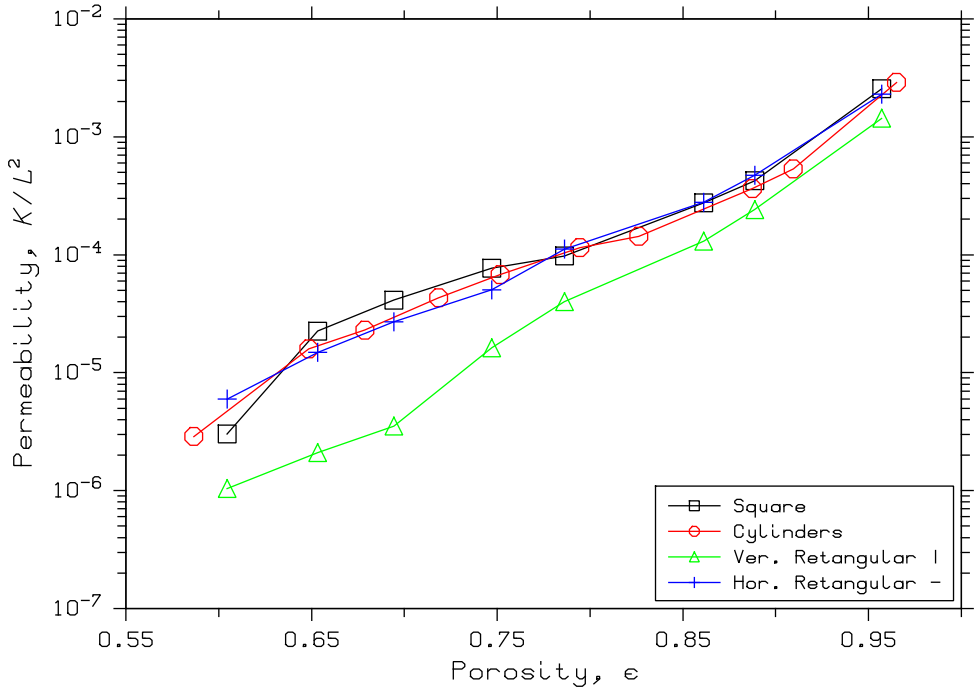

Figure 7: Results for permeability in disordered porous media.

4. Conclusion

Here, the permeability for ordered and disordered porous media is calculated using the lattice Boltzmann method with two relaxation time parameters for the collision operator. Initially, the permeability predicted by the TRT model is compared to the results for the BGK model for the flow along a bunch of channels formed by parallel flat plates. It is shown that the TRT model returns the same value of permeability for different values of viscosity, while the permeability calculated by the BGK model depends on the value of viscosity. Then, the flow in ordered porous media formed by aligned arrangement of parallel cylinders is solved and the results are compared to correlations. Finally the flow in random porous media formed by particles with different cross-sections is solved to determine the effect of particle shape and orientation on permeability.

The results for aligned cylinders are compared to solutions from other authors available in the literature, showing excellent agreement for the range of porosity of validity of their results. The simulations with LBM-TRT extended the previous results up to the limit of percolation of the fluid phase.

The results for disordered porous media are basically independent of the shape of the solid cylinders, as long as the medium remains isotropic. The largest difference is observed between the results for the vertical and horizontal plate cross section. The anisotropy of the porous structures results in different flow configurations for the alligned and the transversal arrangement of plates. The porous media with plate like cylinders result in an anisotropic permeability tensor.

5. Acknowledgments

The authors acknowledge the financial support of the PRH09-ANP/MCT for the leading author. The authors also thank the many comments by Prof. P. C. Phillipi and his group at UFSC.

6. References

Abe, T., 1997. "Derivation of the lattice boltzmann method by means of the discrete ordinate method for the boltzmann equation". *Journal of Computational Physics*, Vol. 131, pp. 241–247.

Belov, E.B., Lomov, S.V., Verpoest, I., Peters, T., Roose, D., Parnas, R.S., Hoes, K. and Sol, H., 2004. "Modelling of permeability of textile reinforcements: lattice boltzmann method". *Composities Science and Technology*, Vol. 64, pp. 1069–1080.

Bhatnagar, P.L., Gross, E.P. and Krook, M., 1954. "A model for collision processes in gases. i. small amplitude processes in charged and neutral one-component systems". *Physical Review*, Vol. 94, No. 3, pp. 511–525.

Boutin, C. and Geindreau, C., 2008. "Estimates and bounds of dynamic permeability of granular media". *J. Acoust. So. Am*, Vol. 124, pp. 3576–3593.

Clague, D.S., Kandhai, B.D., Zhang, B.D. and Sloot, P.M.A., 2000. "Hydraulic permeability of (un)bounded fibrous media using the lattice boltzmann method". *Physical Review E*, Vol. 61, pp. 616–625.

d'Humières, D. and Ginzburg, I., 2009. "Viscosity independent numerical errors for lattice boltzmann models: From recurrence equations to ŚŚmagicŠŠ collision numbers". *Computers and Mathematics with Applications*, Vol. 58, p. 823Ű840.

Dullien, F.A.L., 1979. *Porous media : fluid transport and pore structure*. Academic Press.

Eidsath, A., Carbonell, R.G., Whitaker, S. and Herrmann, L.R., 1983. "Dispersion in pulsed systems iii: Comparison between theory and experiment for packed beds". *Chem. Eng. Sci.*, Vol. 38, pp. 1803–16.

Ginzburg, I. and d'Humières, D., 2003. "Multireflection boundary conditions for lattice boltzmann models". *Phisical Review E*, Vol. 68, p. 066614.

He, X. and Luo, L., 1997. "Theory of the lattice boltzmann method: From the boltzmann equation to the lattice boltzmann equation". *Physical Review E*, Vol. 56, No. 6, pp. 6811–6817.

Kaviany, M., 1995. *Heat Transfer in Porous Media*. Springer, 2nd edition.

Lee, S.L. and Yang, J.H., 1997. "Modeling of darcy-forchheimer drag for fluid flow across a bank of circular cylinders". *International Journal of Heat and Mass Transfer*, Vol. 40, pp. 3149–3155.

Manwart, C., Aaltosalmi, U., Koponem, A., Hilfer, R. and Timonen, J., 2002. "Lattice-boltzmann and finite-difference simulations for permeability for three-dimensional porous media". *Physical Review E*, Vol. 66, p. 016702.

McNamara, G.R. and Zanetti, G., 1988. "Use of the boltzmann equation to simulate lattice-gas automata". *Physical Review Letters*, Vol. 61, No. 20, pp. 2332–2335.

Mityushev, V. and Adler, P.M., 2002. "Longitudinal permeability of spatially periodic rectangular arrays of circular cylinders i. a single cylinder in the unit cell". *Z. Angew. Math. Mech.*, Vol. 82, pp. 335–345.

Nabovati, A., Llewellin, E.W. and Sousa, A.C., 2009. "A general model for the permeability of fibrous porous media based on fluid flow simulations using the lattice boltzmann method". *Composities: Part A*, Vol. 40, pp. 860–869.

Noble, D.R., Chen, S., Georgiadis, J.G. and Buckius, R.O., 1995. "A consistent hydrodynamic boundary condition for the lattice boltzmann method". *Phys. Fluids*, Vol. 7, No. 1, pp. 203–9.

Pan, C., Luo, L.S. and Miller, C.T., 2006. "An evaluation of lattice boltzmann schemes for porous medium flow simulation". *Computers & Fluids*, Vol. 35, p. 898Ű909.

Petrasch, J., Meier, F., Friess, H. and Steinfeld, A., 2008. "Tomography based determination of permeability, dupuit-forchheimer coefficient, and interfacial heat transfer coefficient in reticulate porous ceramics". *International Journal of Heat and Fluid Flow*, Vol. 29, pp. 315–326.

Philippi, P.C., Hegele, L.A., dos Santos, L.O.E. and Sumas, R., 2006. "From the continuous to the lattice boltzmann equation: The discretization problem and thermal models". *Physical Review E*, Vol. 73, p. 056702.

Sadiq, T.A.K., Advani, S.G. and Parnas, R.S., 1995. "Experimental investigation of transverse flow through aligned cylinders". *International Journal of Multiphase Flow*, Vol. 21, pp. 755–774.

Sahraoui, M. and Kaviany, M., 1994. "Slip and no-slip temperature boundary conditions at the interface of porous, plain media: convection". *International Journal of Heat and Mass Transfer*, Vol. 37, pp. 1029–1044.

Sangani, A.S. and Acrivos, A., 1982. "Slow flow past periodic arrays of cylinders with application to heat transfer". *International Journal of Multiphase Flow*, Vol. 8, pp. 193–206.

Santos, L., Philippi, P., Damiani, M.C. and Fernandes, C.P., 2002. "Using three-dimensional reconstructed microstructures for predicting intrinsic permeability of reservoir rocks based on a boolean lattice gas method". *Journal of Petroleum Science and Engineering*, Vol. 35, pp. 109–124.

Scheidegger, A.E., 1974. *The physics of flow through porous media*. University of Toronto Press.

Shan, X., Yuan, X. and Chen, H., 2006. "Kinetic theory representation of hydrodynamics: a way beyond the navier-stokes equation". *Journal of Fluid Mechanics*, Vol. 550, pp. 413–441.

Sobera, M.P. and Kleijn, C.R., 2006. "Hydraulic permeability of ordered and disordered single-layer arrays of cylinders". *Physical Review E*, Vol. 74, p. 036301.

Tamayol, A. and Bahrami, M., 2009. "Analytical determination of viscous permeability of fibrous porous media". *International Journal of Heat and Mass Transfer]*, Vol. 52, pp. 2407–2414.

Torquato, S., 1990. "Bounds on thermoelastic properties of suspensions of spheres". *Journal of Applied Physics*, Vol. 67, p. 7223.

Torquato, S. and B. Lu, B., 1990. "Rigorous bounds on the fluid permeability : Effect of polydispersivity in grain size". *Physics of Fluids A*, Vol. 2, p. 487.

Torquato, S. and Beasley, J.D., 1997. "Bounds on the permeability of a random array of partially penetrable spheres". *Phys. Fluids*, Vol. 30, pp. 633–641.

Wang, C.Y., 1996. "Stokes flow through an array of rectangular fibers". *International Journal of Multiphase Flow*, Vol. 22, pp. 185–194.

Wang, C.Y., 2001. "Stokes flow through a rectangular array of circular cylinders". *Fluid Dynamics Research*, Vol. 29, pp. 65–80.

Wang, J., Leung, C. and Chow, Y., 2003. "Numerical solutions for flow in porous media". *Int. J. Numer. Anal. Meth. Geomech.*, Vol. 27, pp. 565–583.

Zou, Q. and He, X., 1997. "On pressure and velocity flow boundary conditions and bounceback for the lattice boltzmann bgk model". *Physics of Fluids*, Vol. 9, No. 6, pp. 1591–1598.

7. Responsibility notice

The author(s) is (are) the only responsible for the printed material included in this paper